ARTICLES

Chromatin remodelling at promoters suppresses antisense transcription

Iestyn Whitehouse[1], Oliver J. Rando[3], Jeff Delrow[2] & Toshio Tsukiyama[1]

Chromatin allows the eukaryotic cell to package its DNA efficiently. To understand how chromatin structure is controlled across the *Saccharomyces cerevisiae* genome, we have investigated the role of the ATP-dependent chromatin remodelling complex Isw2 in positioning nucleosomes. We find that Isw2 functions adjacent to promoter regions where it repositions nucleosomes at the interface between genic and intergenic sequences. Nucleosome repositioning by Isw2 is directional and results in increased nucleosome occupancy of the intergenic region. Loss of Isw2 activity leads to inappropriate transcription, resulting in the generation of both coding and noncoding transcripts. Here we show that Isw2 repositions nucleosomes to enforce directionality on transcription by preventing transcription initiation from cryptic sites. Our analyses reveal how chromatin is organized on a global scale and advance our understanding of how transcription is regulated.

Nucleosomes are the basic repeating units of chromatin. They are composed of an octamer of histone proteins around which DNA is tightly wrapped[1]. The DNA contained within nucleosomes is less accessible than linker DNA; as a result, processes that rely on access to the genome are influenced profoundly by the positions of nucleosomes along DNA[2]. However, little is known about the factors that govern nucleosome positioning *in vivo*.

One factor governing nucleosome positioning is the intrinsic DNA sequence preference for the histone octamer, and sequences that favour and disfavour nucleosome assembly have been described[3–5]. Recent genomic studies have used intrinsic sequence preferences to predict nucleosome positions across a genome on the basis of DNA sequence[6,7] with modest success—*in vivo* nucleosome positions are predicted well for only a subset of genomic loci. This probably reflects the fact that a variety of protein factors also contribute to nucleosome positioning *in vivo*. Principal among these are ATP-dependent chromatin remodelling enzymes that alter the positions of nucleosomes *in vivo* and *in vitro*[8]. Therefore, to understand how nucleosome positions are specified *in vivo*, it is important to understand not only the contribution made by the DNA sequence but also the role of factors such as chromatin remodelling enzymes[9].

Isw2 is one such ATP-dependent chromatin remodelling enzyme, and belongs to a family of proteins that are highly evolutionarily conserved[10,11]. In multicellular eukaryotes, Isw2 homologues have been implicated in the regulation of transcription[12,13], global chromosome structure[14], DNA replication[15,16], cell cycle progression[17], ribosomal DNA silencing[18,19] and cohesin loading[20]. In budding yeast, Isw2 acts as a gene repressor[21–23] by overriding the underlying nucleosome positioning signals of DNA[24], repositioning nucleosomes over unfavourable DNA sequences to establish a chromatin configuration that is repressive to transcription.

To understand global Isw2 function, we used high-resolution tiled microarrays to map the positions of nucleosomes across the yeast genome, and defined how their positioning is altered in a Δ*isw2* mutant strain. Nucleosome repositioning by Isw2 is directional and results in compact chromatin adjacent to sites of transcriptional activity. Loss of Isw2 leads to nucleosome positional changes and inappropriate transcription, resulting in the generation of noncoding transcripts. We find that chromatin remodelling is an important process that prevents aberrant transcription of the genome.

Genome-wide analysis of Isw2-dependent chromatin remodelling

We sought to discover Isw2 targets across the yeast genome by identifying nucleosomes whose positioning is altered in a Δ*isw2* mutant strain. We purified nucleosomal DNA from both wild-type and Δ*isw2* mutant yeast, and hybridized each to high-resolution tiled microarrays[25] that cover the entire yeast genome with ~5 base pair (bp) spacing (Supplementary Fig. 2).

Nucleosome-sized peaks were found across the genome; arrays of positioned nucleosomes generate a periodic signal whose maxima and minima are separated by the nucleosome repeat length of 165 bp. Comparison of wild-type nucleosome locations with those from a Δ*isw2* mutant revealed many sites of altered nucleosome positioning. To systematically identify these regions, we developed a comparative approach to detect differences in nucleosomal positioning and/or occupancy between wild-type and Δ*isw2* mutant strains (Supplementary Fig. 3). This analysis identified >1,000 distinct regions, typically of ~600 bp in length, where chromatin structure was disrupted in the Δ*isw2* mutant (Fig. 1 and Supplementary Table 1).

Having established the locations of chromatin changes, we used chromatin immunoprecipitation (ChIP) in conjunction with the

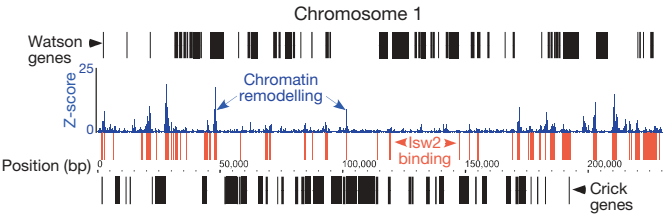

Figure 1 | Definition of Isw2 function using high-density microarrays. Shown is the global view of Isw2 binding and chromatin remodelling. Data for chromosome 1 are shown as an example. Black boxes represent ORFs, red boxes represent sites of Isw2(K215R) enrichment (Isw2 targets), and the blue line indicates sites of altered chromatin structure in an Δ*isw2* mutant.

[1]Division of Basic Sciences, [2]Genomics Resource, Fred Hutchinson Cancer Research Center, Seattle, Washington 98109, USA. [3]Department of Biochemistry and Molecular Pharmacology, University of Massachusetts Medical School, Worcester, Massachusetts 01605, USA.

tiled microarrays to determine whether Isw2 was acting directly at these loci. Previously we found that the sites bound by a catalytically inactive mutant of the Isw2 protein, Isw2(K215R), are a reliable indicator of functional Isw2 targets, whereas the wild-type protein binds nonspecifically across the genome[26]. We therefore defined sites of Isw2 binding as sites at which Isw2(K215R) is enriched relative to the wild-type control. Figure 1 shows the sites of Isw2(K215R) binding and nucleosome positional changes across chromosome 1. Comparison of Isw2 localization with sites of Isw2-dependent nucleosome positional changes shows a tight association (Supplementary Fig. 4), suggesting that Isw2 is directly responsible for most of the chromatin changes we identify.

We then asked whether Isw2 is preferentially targeted to particular regions of the genome. Isw2 targets were divided into groups reflecting their proximity to genomic features (Supplementary Table 1). Isw2 function was detected at the 5′ ends of genes, as well as upstream of transfer RNA genes, consistent with previous reports[21,23,26,27]. In addition, we detected Isw2 activity at the 3′ end of genes and in intergenic regions distal to known genomic features. Examples of Isw2-dependent nucleosome repositioning at individual loci are shown in Supplementary Fig. 5.

Nucleosome repositioning at the 5′ end of genes

Isw2 is targeted to the 5′ end of ~20% of genes transcribed by RNA polymerase II, and Isw2-dependent chromatin remodelling was detected at ~35% of these targets (Supplementary Table 1). Because loss of Isw2 function at the 5′ end of genes is generally correlated with transcriptional derepression[21,23,27], chromatin structure changes mediated by Isw2 probably act to repress transcription at these sites. To define common features of Isw2-mediated nucleosome repositioning at the 5′ ends of genes, we aligned 5,767 non-dubious genes according to the midpoint of the first defined nucleosome (+1) upstream of the coding region of the gene (Fig. 2a). We first analysed the distribution of wild-type nucleosome positions, because previous high-resolution studies have only covered a fraction of the yeast genome[25,28]. Nucleosomes are highly organized at the 5′ end of genes and this organization spreads into the adjacent coding sequence. A short nucleosome-free region (NFR, which varies in size from gene to gene) typically lies upstream of nucleosome +1 (the first nucleosome upstream of the translation start site), and is the predominant site for transcription-factor-binding at promoters[25] (Fig. 2 and Supplementary Fig. 16b). The transcription start site is commonly downstream of the transcription-factor-binding sites and is generally occluded by the first half of nucleosome +1, consistent with recent analysis[28].

We then turned to the chromatin structure of Δ*isw2* mutants, asking if any general rules could be formulated for the action of Isw2 at the 5′ ends of genes. We selected genes that are enriched for Isw2 and display Isw2-dependent chromatin remodelling (~400 genes), and then aligned these loci according to the position of the +1 nucleosome determined for wild-type yeast. Next we overlaid the nucleosome hybridization signal from wild-type nucleosomes to generate an intensity map, the darkness of which is proportional to the number of traces at that coordinate; the average of the signal is shown as a green line (Fig. 3a). We generated a similar map for nucleosomes harvested from Δ*isw2* mutant yeast (Fig. 3b). To determine nucleosome repositioning trends at Isw2 targets, we calculated the difference between the wild-type and Δ*isw2* mutant intensity maps (Fig. 3c). This demonstrated a clear bias in nucleosome repositioning in the Δ*isw2* mutant strain. Specifically, there is a directional shift in the population of nucleosomes away from the NFR/intergenic region towards the adjacent genic sequence in Δ*isw2* mutants (Fig. 3c and Supplementary Fig. 6a, b). The size of the shift ranges up to ~70 bp, with a typical shift of ~15 bp that decreases in size for each successive nucleosome (Supplementary Fig. 7). Because loss of Isw2 function leads to a shift in nucleosomes away from the intergenic region, this finding implies that Isw2 functions to increase nucleosome occupancy at intergenic regions at the 5′end of genes by repositioning nucleosomes.

Nucleosome repositioning at the 3′end of genes

Nucleosome positional changes are also evident at the 3′ends of ~250 genes that are bound by the Isw2(K215R) protein (Supplementary Table1). We studied these targets by aligning the 3′ends of genes with respect to the nucleosome closest to the end of the open reading frame (ORF). We then compared how nucleosomes are repositioned at Isw2 targets and non-targets as described above. Again, we observe a distinct bias in the directionality of shifting; like at the 5′ end of genes, loss of Isw2 results in a shift of nucleosomes away from the intergenic region (Fig. 3f, and Supplementary Figs 6c, d and 7).

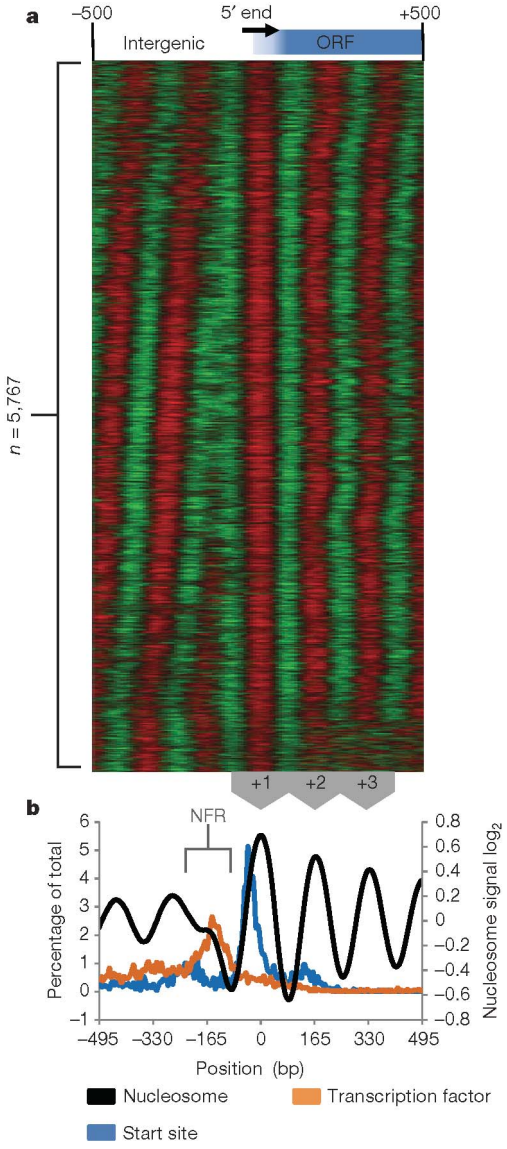

Figure 2 | Distinct nucleosome organization at the 5′ end of genes. **a**, A self-organizing map of nucleosome order at the 5′ end of genes. The 5′ ends of 5,767 non-dubious ORFs were aligned according to the +1 nucleosome adjacent to a short NFR. Loci with similar nucleosome arrangements are placed next to each other. Red represents a positive signal, whereas green is negative. **b**, The signal from **a** is averaged to illustrate typical nucleosome positions, shown as a black line. A frequency plot of the transcription start site from ref. 46 and the predicted transcription-factor-binding sites (with the most stringent cut-offs) from ref. 47 are displayed in blue and orange, respectively. Transcription factors typically bind within the NFR, whereas the transcription start site lies within the 5′end of the +1 nucleosome.

Thus, at both the 5′ and the 3′ ends of genes, Isw2 serves to shift nucleosomes onto adjacent intergenic regions.

Isw2 action at the 3′ ends of genes represents a major and previously unidentified class of targets. To characterize this group of targets more closely, we analysed their arrangement with respect to adjacent genomic features. In general, the intergenic region downstream of an ORF can be either convergent (containing the 3′ ends of two converging genes) or tandem (containing the 3′ end of the gene followed by the 5′ promoter of the adjacent gene). Our analysis revealed that more than 75% of the intergenic regions downstream of 3′ Isw2 targets are tandem, which is significantly higher than the genomic average of ~48%. Therefore, Isw2 activity at these targets seems to be correlated with the presence of an adjacent gene promoter. The high resolution of our analysis allows us to identify unambiguously the 3′ end of genes as a unique class of targets, rather than an artefact of Isw2 action at the 5′ end of the downstream gene (Fig. 4 and Supplementary Fig. 8).

Isw2 suppresses non-coding, antisense transcription

Because ~90% of all Isw2 targets are found adjacent to gene promoter regions, we considered a model in which Isw2 functions to repress transcription from promoters in general. According to this model, loss of Isw2 at the 5′ end of genes leads to increased transcription of the coding sequence. In contrast, loss of Isw2 action at the 3′ end of a gene would result in a shift in the nucleosome upstream of the NFR relative to the 5′ end of the adjacent gene. We reasoned that this might permit incorrectly oriented transcription to proceed from the adjacent promoter, resulting in the production of a noncoding, antisense transcript (Supplementary Fig. 1).

We sought direct evidence for the production of noncoding transcripts in yeast lacking Isw2. However, many noncoding transcripts are rapidly degraded by the exosome[29], complicating the search for these transcripts. A key component of this pathway is the poly(A) polymerase Trf4 (also known as Pap2); this polyadenylates transcripts, thereby targeting them for degradation[30–34]. We therefore generated a strain in which both *ISW2* and *TRF4* were deleted. The double-mutant strain displayed a synthetic slow growth phenotype that was more severe than either of the single mutants (Supplementary Fig. 9). This finding confirms previous results from high-throughput studies[35] and supports the idea that Isw2, like Trf4, has a critical role in the suppression of aberrant transcription.

To assay directly the presence of noncoding transcripts, we performed strand-specific northern analysis for a subset of genes in which Isw2 functions at the 3′ end. At each of the loci tested, we found that deletion of *ISW2* in a *trf4* background results in the generation of noncoding-antisense transcripts (Fig. 4a–c). At the gene *YGR166W* we found that production of a noncoding transcript is primarily dependent on the lack of Isw2 alone, whereas deletion of *TRF4* does influence transcript length (Fig. 4c). We used primer extension to determine the start site of the transcripts, and found that they are initiated at the 3′ end of the gene (Fig. 4 and Supplementary Fig. 10). We analysed the location of the antisense transcripts by use of high-resolution microarrays, and confirmed nucleosome repositioning by Southern blots (Supplementary Fig. 11). We also asked if noncoding transcripts are produced from other classes of Isw2 targets. At two loci—upstream of the tRNA gene *tT(UGU)G1*, and at an intergenic region, *iYDL025C*—we found evidence of noncoding transcription when both *ISW2* and *TRF4* are deleted (Supplementary Fig. 12). These results indicate a general role for Isw2 in the repression of noncoding transcription.

Discussion

Our studies provide a picture of how an ATP-dependent chromatin remodelling complex controls chromatin structure across a genome. We find that Isw2 functions at the interface between genic and intergenic regions, where it catalyses the directional shift of nucleosomes towards intergenic regions. Our data illustrate how nucleosomes are organized at regulatory sequences and how nucleosome repositioning is used to repress transcription from intergenic regions.

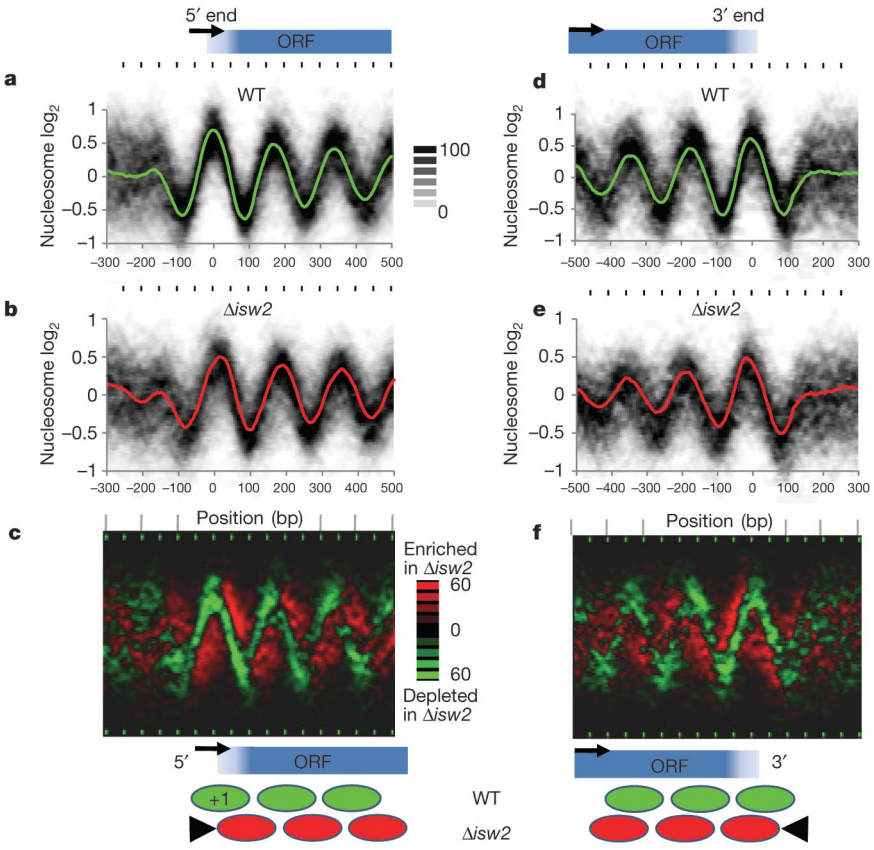

Figure 3 | Loss of Isw2 leads to directional nucleosome repositioning at the 5′ end and 3′ end of genes. **a**, **d**, Intensity maps of the nucleosomal signal at Isw2 targets at the 5′ end (**a**) and the 3′ end (**d**) of genes in wild-type (WT) cells. The average signal is shown as a green line. **b**, **e**, This is as described in **a** and **d** except using data from Δ*isw2* mutant yeast; the average signal is shown as a red line. **c**, **f**, Intensity maps showing nucleosome positional changes at Isw2 targets. Data from **a** were subtracted from that of **b** to generate **c**. Data from **d** were subtracted from that of **e** to generate **f**. Green represents regions that are depleted in an Δ*isw2* mutant strain, whereas red represents regions that are enriched. Nucleosome positional changes by Isw2 at 5′ and 3′ targets are illustrated at the bottom. The grey and colour scales represent the percentage of signal that is below that intensity. Black and green ticks are placed at 50-bp intervals.

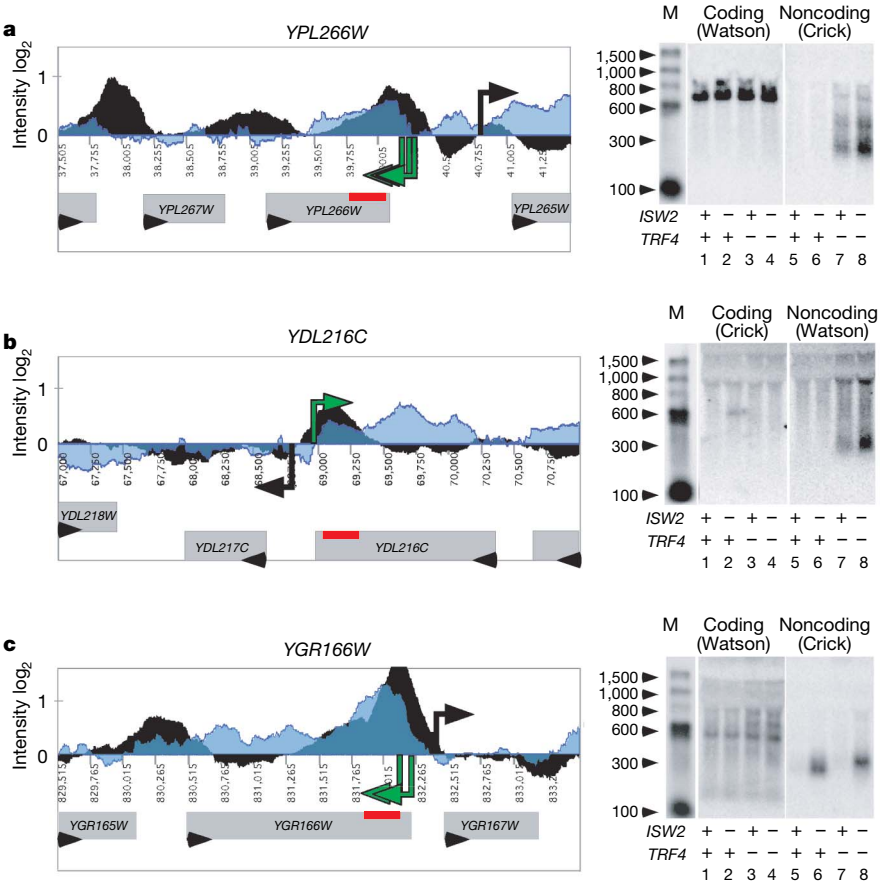

Figure 4 | Loss of Isw2 leads to noncoding transcription at the 3′ end of genes. Left, microarray data for Isw2 ChIP and RNA analyses. Log_2 ratio of the double mutant Δ*isw2* Δ*trf4* versus Δ*trf4* RNA signal is shown in transparent blue; Isw2(K215R) enrichment is shown in black. ORFs are shown as grey boxes, transcriptional direction is shown as a black arrow, and the location of northern blot probes used are shown as a red bar. Principal transcriptional start sites of the noncoding transcripts are shown as extended green arrows; start sites of coding transcripts mapped in ref. 48 are shown as extended black arrows. Right, strand-specific northern blots of Isw2 3′ targets. Loss of *ISW2* and *TRF4* results in the generation of noncoding-antisense transcripts at the genes *YPL266W* (**a**) and *YDR216C* (**b**); deletion of *ISW2* alone results in noncoding-antisense transcripts from the gene *YGR166W* (**c**). M, molecular weight marker.

We find that the positioning of thousands of nucleosomes adjacent to important regulatory sequences is controlled by Isw2. Yeast promoters frequently contain AT-rich DNA sequences[36] that have been found to inhibit nucleosome positioning[5,37,38]. Because Isw2 is able to use the energy from ATP hydrolysis to override the inherent nucleosome-positioning signal of the underlying DNA[24], Isw2 may function generally to reposition nucleosomes on unfavourable DNA sequences. Consistent with this, we find that poly dA/dT tracts, which are highly enriched at NFRs[25], are located within nucleosome +1 at many Isw2 targets (Supplementary Fig. 13). Loss of Isw2 would allow nucleosomes to adopt their inherent positioning preference, uncovering canonical or cryptic sites for transcriptional initiation. Because transcription is not necessary for the nucleosome positional changes caused by Isw2 deletion (Supplementary Fig. 14), transcription is likely to be a consequence rather than a cause of nucleosome repositioning at Isw2 targets. The broad scope of Isw2 action has implications for predictions of nucleosome positions on the basis of DNA sequence alone[6,7]. These studies have had some success, but at present they are unable to predict accurately many nucleosome positions within the cell[28] (Supplementary Fig. 15). The ability of proteins such as Isw2 to reposition nucleosomes provides a clear illustration that cellular factors actively operate to disrupt the intrinsic cues that would otherwise package the genome.

The primary site of action of Isw2 at the 5′ end of genes is the +1 nucleosome. This nucleosome is positioned such that the transcription start site is occluded by its 5′ edge[28] (Fig. 2). Upstream of +1 generally lies a short NFR, which typically contains transcription-factor-binding sites[25,28] (Fig. 2, Supplementary Fig. 16) and is probably the site for preinitiation-complex assembly. The nucleosome +1 generally contains the variant histone Htz1 (refs 28 and 39–41; Supplementary Fig. 17), which marks genes for rapid reactivation[42] and is subject to rapid replication-independent turnover[43]. This nucleosome is likely to act as a principal regulator of transcription, because RNA polymerase cannot reach the coding sequence without first transiting +1. In the context of this study, the specificity of Isw2 for this 'gatekeeper' nucleosome probably provides a regulatory mechanism to control gene expression by occluding the transcription start site or regulatory sequences through nucleosome repositioning (Supplementary Fig. 1).

A key finding of this study is that transcription is able to initiate from cryptic start sites when *ISW2* is deleted, which results in inappropriately oriented transcription from intergenic regions. This result is important because the mechanisms that ensure that transcription occurs in the correct orientation are largely unknown. Our findings suggest a model in which promoters are not intrinsically directional and can support inappropriately oriented transcription when chromatin structure is perturbed (Supplementary Fig. 1). Thus, transcription factors and DNA sequence alone are insufficient to prevent initiation from cryptic sites at these promoters. Because Isw2 remodels chromatin structure at the 3′ ends of many genes, the control of transcription by nucleosome positioning may be a general mechanism used by the cell.

METHODS SUMMARY

All yeast strains (S288C) were grown to mid-log phase ($D_{600} = 0.7$). Chromatin was crosslinked by the addition of formaldehyde, and was digested to mononucleosomes using micrococcal nuclease (MNase) and exonuclease III. Mononucleosomal DNA was purified by agarose gel electrophoresis. For microarrays, all samples were hybridized to *S. cerevisiae* tiling 1.0R arrays (Affymetrix). The signals from perfect match oligonucleotides were used to determine relative chromatin structure changes (Fig. 1, Supplementary Fig. 3); the difference between the hybridization signal from wild-type fragmented nucleosomal DNA and Δ*isw2* fragmented nucleosomal DNA was calculated. To determine nucleosome positions, the hybridization signal from fragmented nucleosomal DNA was normalized to the signal from full-length nucleosomal DNA. To align nucleosomes at the 5′ end of genes we first aligned all non-dubious ORFs according to the translation start site. These were then grouped using K-means clustering into ten nodes using Cluster[44]. Each node was manually aligned with respect to the nucleosome directly upstream of the NFR; if an

NFR was not apparent, we chose the first nucleosome upstream of the translation start site. This nucleosome was designated as +1. The data were further aligned by iteratively fitting an idealized nucleosome signal to the data. Signals with the best fit to the idealized nucleosome were defined as nucleosomes. Nucleosomes were organized at the 3′ end of genes in a similar manner to that at the 5′ ends. In this case the first nucleosome 5′ of the stop codon was chosen. For ChIP, all proteins were 3× Flag-tagged. Chromatin from Isw2 and Isw2(K215R) was fragmented using MNase as described in ref. 45; the immunoprecipitation method is described in ref. 26. Each immunoprecipitation sample is normalized to an input sample to control for experimental variations. For RNA analysis, yeast were grown to mid-log phase and the RNA was extracted with the use of acid phenol. Processed and raw data are available at http://www.fhcrc.org/science/labs/tsukiyama/supplemental_data/Global_Nuc_mapping.html.

Full Methods and any associated references are available in the online version of the paper at www.nature.com/nature.

Received 6 July; accepted 18 October 2007.

1. Luger, K., Mader, A. W., Richmond, R. K., Sargent, D. F. & Richmond, T. J. Crystal structure of the nucleosome core particle at 2.8 Å resolution. *Nature* **389,** 251–260 (1997).
2. Ehrenhofer-Murray, A. E. Chromatin dynamics at DNA replication, transcription and repair. *Eur. J. Biochem.* **271,** 2335–2349 (2004).
3. Satchwell, S. C., Drew, H. R. & Travers, A. A. Sequence periodicities in chicken nucleosome core DNA. *J. Mol. Biol.* **191,** 659–675 (1986).
4. Lowary, P. T. & Widom, J. New DNA sequence rules for high affinity binding to histone octamer and sequence-directed nucleosome positioning. *J. Mol. Biol.* **276,** 19–42 (1998).
5. Anderson, J. D. & Widom, J. Poly(dA-dT) promoter elements increase the equilibrium accessibility of nucleosomal DNA target sites. *Mol. Cell. Biol.* **21,** 3830–3839 (2001).
6. Segal, E. *et al.* A genomic code for nucleosome positioning. *Nature* **442,** 772–778 (2006).
7. Ioshikhes, I. P., Albert, I., Zanton, S. J. & Pugh, B. F. Nucleosome positions predicted through comparative genomics. *Nature Genet.* **38,** 1210–1215 (2006).
8. Narlikar, G. J., Fan, H. Y. & Kingston, R. E. Cooperation between complexes that regulate chromatin structure and transcription. *Cell* **108,** 475–487 (2002).
9. Rando, O. J. & Ahmad, K. Rules and regulation in the primary structure of chromatin. *Curr. Opin. Cell Biol.* **19,** 250–256 (2007).
10. Eisen, J. A., Sweder, K. S. & Hanawalt, P. C. Evolution of the SNF2 family of proteins: subfamilies with distinct sequences and functions. *Nucleic Acids Res.* **23,** 2715–2723 (1995).
11. Flaus, A., Martin, D. M., Barton, G. J. & Owen-Hughes, T. Identification of multiple distinct Snf2 subfamilies with conserved structural motifs. *Nucleic Acids Res.* **34,** 2887–2905 (2006).
12. Badenhorst, P., Voas, M., Rebay, I. & Wu, C. Biological functions of the ISWI chromatin remodeling complex NURF. *Genes Dev.* **16,** 3186–3198 (2002).
13. Yasui, D., Miyano, M., Cai, S., Varga-Weisz, P. & Kohwi-Shigematsu, T. SATB1 targets chromatin remodelling to regulate genes over long distances. *Nature* **419,** 641–645 (2002).
14. Deuring, R. *et al.* The ISWI chromatin-remodeling protein is required for gene expression and the maintenance of higher order chromatin structure *in vivo*. *Mol. Cell* **5,** 355–365 (2000).
15. Collins, N. *et al.* An ACF1–ISWI chromatin-remodeling complex is required for DNA replication through heterochromatin. *Nature Genet.* **32,** 627–632 (2002).
16. Poot, R. A. *et al.* The Williams syndrome transcription factor interacts with PCNA to target chromatin remodelling by ISWI to replication foci. *Nature Cell Biol.* **6,** 1236–1244 (2004).
17. Fyodorov, D. V., Blower, M. D., Karpen, G. H. & Kadonaga, J. T. Acf1 confers unique activities to ACF/CHRAC and promotes the formation rather than disruption of chromatin *in vivo*. *Genes Dev.* **18,** 170–183 (2004).
18. Zhou, Y., Santoro, R. & Grummt, I. The chromatin remodeling complex NoRC targets HDAC1 to the ribosomal gene promoter and represses RNA polymerase I transcription. *EMBO J.* **21,** 4632–4640 (2002).
19. Li, J., Langst, G. & Grummt, I. NoRC-dependent nucleosome positioning silences rRNA genes. *EMBO J.* **25,** 5735–5741 (2006).
20. Hakimi, M. A. *et al.* A chromatin remodelling complex that loads cohesin onto human chromosomes. *Nature* **418,** 994–998 (2002).
21. Goldmark, J. P., Fazzio, T. G., Estep, P. W., Church, G. M. & Tsukiyama, T. The Isw2 chromatin remodeling complex represses early meiotic genes upon recruitment by Ume6p. *Cell* **103,** 423–433 (2000).
22. Fazzio, T. G., Gelbart, M. E. & Tsukiyama, T. Two distinct mechanisms of chromatin interaction by the isw2 chromatin remodeling complex *in vivo*. *Mol. Cell. Biol.* **25,** 9165–9174 (2005).
23. Kent, N. A., Karabetsou, N., Politis, P. K. & Mellor, J. *In vivo* chromatin remodeling by yeast ISWI homologs Isw1p and Isw2p. *Genes Dev.* **15,** 619–626 (2001).
24. Whitehouse, I. & Tsukiyama, T. Antagonistic forces that position nucleosomes *in vivo*. *Nature Struct. Mol. Biol.* **13,** 633–640 (2006).
25. Yuan, G. C. *et al.* Genome-scale identification of nucleosome positions in *S. cerevisiae*. *Science* **309,** 626–630 (2005).
26. Gelbart, M. E., Bachman, N., Delrow, J., Boeke, J. D. & Tsukiyama, T. Genome-wide identification of Isw2 chromatin-remodeling targets by localization of a catalytically inactive mutant. *Genes Dev.* **19,** 942–954 (2005).
27. Fazzio, T. G. *et al.* Widespread collaboration of Isw2 and Sin3–Rpd3 chromatin remodeling complexes in transcriptional repression. *Mol. Cell. Biol.* **21,** 6450–6460 (2001).
28. Albert, I. *et al.* Translational and rotational settings of H2A.Z nucleosomes across the *Saccharomyces cerevisiae* genome. *Nature* **446,** 572–576 (2007).
29. Houseley, J., LaCava, J. & Tollervey, D. RNA-quality control by the exosome. *Nature Rev. Mol. Cell Biol.* **7,** 529–539 (2006).
30. Wyers, F. *et al.* Cryptic pol II transcripts are degraded by a nuclear quality control pathway involving a new poly(A) polymerase. *Cell* **121,** 725–737 (2005).
31. LaCava, J. *et al.* RNA degradation by the exosome is promoted by a nuclear polyadenylation complex. *Cell* **121,** 713–724 (2005).
32. Vanacova, S. *et al.* A new yeast poly(A) polymerase complex involved in RNA quality control. *PLoS Biol.* **3,** e189 (2005).
33. Davis, C. A. & Ares, M. Jr. Accumulation of unstable promoter-associated transcripts upon loss of the nuclear exosome subunit Rrp6p in *Saccharomyces cerevisiae*. *Proc. Natl Acad. Sci. USA* **103,** 3262–3267 (2006).
34. Egecioglu, D. E., Henras, A. K. & Chanfreau, G. F. Contributions of Trf4p- and Trf5p-dependent polyadenylation to the processing and degradative functions of the yeast nuclear exosome. *RNA* **12,** 26–32 (2006).
35. Pan, X. *et al.* A DNA integrity network in the yeast *Saccharomyces cerevisiae*. *Cell* **124,** 1069–1081 (2006).
36. Behe, M. J. An overabundance of long oligopurine tracts occurs in the genome of simple and complex eukaryotes. *Nucleic Acids Res.* **23,** 689–695 (1995).
37. Kunkel, G. R. & Martinson, H. G. Nucleosomes will not form on double-stranded RNa or over poly(dA).poly(dT) tracts in recombinant DNA. *Nucleic Acids Res.* **9,** 6869–6888 (1981).
38. Iyer, V. & Struhl, K. Poly(dA:dT), a ubiquitous promoter element that stimulates transcription via its intrinsic DNA structure. *EMBO J.* **14,** 2570–2579 (1995).
39. Raisner, R. M. *et al.* Histone variant H2A.Z marks the 5′ ends of both active and inactive genes in euchromatin. *Cell* **123,** 233–248 (2005).
40. Guillemette, B. *et al.* Variant histone H2A.Z is globally localized to the promoters of inactive yeast genes and regulates nucleosome positioning. *PLoS Biol.* **3,** e384 (2005).
41. Zhang, H., Roberts, D. N. & Cairns, B. R. Genome-wide dynamics of Htz1, a histone H2A variant that poises repressed/basal promoters for activation through histone loss. *Cell* **123,** 219–231 (2005).
42. Brickner, D. G. *et al.* H2A.Z-mediated localization of genes at the nuclear periphery confers epigenetic memory of previous transcriptional state. *PLoS Biol.* **5,** e81 (2007).
43. Dion, M. F. *et al.* Dynamics of replication-independent histone turnover in budding yeast. *Science* **315,** 1405–1408 (2007).
44. Eisen, M. B., Spellman, P. T., Brown, P. O. & Botstein, D. Cluster analysis and display of genome-wide expression patterns. *Proc. Natl Acad. Sci. USA* **95,** 14863–14868 (1998).
45. Liu, C. L. *et al.* Single-nucleosome mapping of histone modifications in *S. cerevisiae*. *PLoS Biol.* **3,** e328 (2005).
46. Zhang, Z. & Dietrich, F. S. Mapping of transcription start sites in *Saccharomyces cerevisiae* using 5′ SAGE. *Nucleic Acids Res.* **33,** 2838–2851 (2005).
47. MacIsaac, K. D. *et al.* An improved map of conserved regulatory sites for *Saccharomyces cerevisiae*. *BMC Bioinformatics* **7,** 113 (2006).
48. Miura, F. *et al.* A large-scale full-length cDNA analysis to explore the budding yeast transcriptome. *Proc. Natl Acad. Sci. USA* **103,** 17846–17851 (2006).

Supplementary Information is linked to the online version of the paper at www.nature.com/nature.

Acknowledgements We thank members of the Tsukiyama and Henikoff laboratories for discussions, R. Basom for help with data analysis, and S. Henikoff, S. Biggins, S. Hahn and T. Owen-Hughes for critical reading of the manuscript. This work was supported by funds from NIGMS and the Leukemia and Lymphoma Society to T.T, from the Burroughs Wellcome Fund and Human Frontier Science Program to O.J.R, and from the NCI to J.D.

Author Contributions Experimental strategy was designed by I.W. and T.T., and experiments were performed by I.W. Preliminary nucleosome mapping was performed in collaboration with O.J.R. Data were analysed by I.W., with technical assistance from J.D. The paper was written by I.W., with assistance from T.T. All authors discussed the results and experiments, and edited the manuscript.

Author Information Raw data are deposited at GEO with accession numbers GSE8813, GSE8814 and GSE8815. Reprints and permissions information is available at www.nature.com/reprints. Correspondence and requests for materials should be addressed to T.T. (ttsukiya@fhcrc.org).

METHODS

Nucleosome harvest. Mononucleosomal DNA was prepared in a manner similar to that described in ref. 25 except nuclei were digested with the addition of ~700 units of MNase (Worthington) and 100 units of exonuclease III (NEB) for 20 min at 37 °C with constant agitation. Reactions were stopped with the addition of solution S (5% SDS, 100 mM EDTA). RNA and proteins were removed with RNaseA and proteinase K. Crosslinks were reversed by incubation at 65 °C for 16 h. SDS was precipitated from the solution with the addition of 3 M potassium acetate, pH 5.5 (to a final concentration of 750 mM), followed by centrifugation at 4,000*g*. DNA fragments were harvested from the supernatant using a G500 genomic column (Qiagen) according to instructions. DNA was then resolved on a 1.7% agarose gel, and the band corresponding to mononucleosomal DNA excised. Before labelling, full-length nucleosomal DNA fragments were treated with calf intestinal phosphatase (NEB) to remove 3′ phosphates.

Nucleosome data analysis. Nucleosome mapping data was normalized using quantile normalization, and was analysed using TAS software (version 1.1) provided by Affymetrix. We performed two sample analyses, in which there are two data sets termed a treatment and a control group. Each group consists of the subset of data falling within a bandwidth of 33 bp, resulting in n_t treatment probe intensities and n_c control probe intensities. Analysis at a particular position is based on all data aligning within ±1 bandwidth of the position. An estimate of fold enrichment of probes within the bandwidth is calculated using the Hodges–Lehmann estimator associated with the Wilcoxon rank-sum test.

Detection of Isw2-dependent chromatin remodelling. For global chromatin remodelling analysis (Fig. 1 and Supplementary Fig. 3), two biological replicates of wild-type fragmented nucleosomes were defined as the treatment group and two biological replicates of Δ*isw2* fragmented nucleosomes were defined as the control group using Tiling Analysis Software (TAS). The resulting $\log_2$ transformed signal was then spaced evenly at 5-bp intervals across the genome. Nucleosome-sized signals, S^n, were calculated by applying the following function at 5-bp intervals to the data set: $S_i^n = S_i(S_{i+165} + S_{i-165})$, where S corresponds to the signal at the chromosomal coordinate i. We defined sites of chromatin remodelling as 'blocks' whose signal is above 93% of the overall signal; this value was chosen because it gave the best correlation with Isw2(K215R) binding. Blocks less than 100 bp apart were classified as the same block.

Nucleosome signal normalization. To generate nucleosome signals, we initially fragmented the nucleosomal DNA into ~50-bp pieces and normalized its signal to that of DNaseI-digested genomic DNA. Nucleosome positions generated by this approach were highly consistent with previously published data (Supplementary Fig. 18). During our analysis, we found that nucleosome signals are highly dependent on the length of the DNA fragment that is hybridized to the microarray. Ends of full-length nucleosomal DNA fragments (~150 bp) from well-positioned nucleosomes hybridize with a ~2-fold greater efficiency than the mid points of the fragments. This is probably a steric effect caused by the relatively short length of oligonuclotides on the microarray. We find that the signal from these full-length nucleosomal DNA fragments provides an accurate means of identifying the ends of the nucleosomal DNA fragments (Supplementary Fig. 18). We found that nucleosome mapping could be improved significantly by generating a composite signal by using the data from fragmented nucleosomes to identify nucleosome peaks and by using the data from full-length nucleosomes to identify nucleosome edges. We found that normalizing the hybridization signal for fragmented nucleosomal DNA to that of full-length nucleosomal DNA generated an accurate nucleosome map that had better definition of nucleosomes than the signal generated from fragmented nucleosomes alone. Data normalized in this way were used in this paper; however, essentially the same results were obtained by normalizing the signals from fragmented nucleosomes to that of DNaseI-digested genomic DNA. Detrending was performed on the nucleosome hybridization data. This was done in a sliding window by subtracting the mean (of the maximum and minimum values over a 40 probe, ~200 bp, window) from the normalized data.

Nucleosome positional analysis. For nucleosome positional analysis, two biological replicates of wild-type fragmented nucleosomes were defined as the treatment group and two different biological replicates of wild-type full-length nucleosomes were defined as the control group. For nucleosome positioning in Δ*isw2* mutant yeast, two biological replicates of Δ*isw2* fragmented nucleosomes were defined as the treatment group and two different biological replicates of Δ*isw2* full-length nucleosomes were defined as the control group. Probe positions were set to the 3′ end of the oligonucleotide because this gave best correlation with published data sets. Nucleosome positions were determined by iteratively fitting an idealized nucleosome signal to a data set. The data set was first evenly spaced at 5-bp intervals and the probe position with the best fit (calculated by the Pearson correlation coefficient) to the idealized nucleosome signal was defined as the dyad. Figure 3 was created by aligning signals to a common point (+1 at the 5′ end or the nucleosome closest to the 3′ end of the gene), and then the frequency of nucleosome signal intensities was calculated at 5-bp intervals.

Generation of fragmented nucleosome DNA. Mononucleosomal DNA (3 μg) was placed in a 50 μl reaction containing 50 mM Tris:Cl, pH 6.8, 5 mM $MgCl_2$ and 0.3 μg μl^{-1} random hexamers. The reaction was incubated at 95 °C for 5 min, and was then chilled rapidly on ice. Five microlitres of dNTP mix (1.2 mM dGTP, 1.2 mM dCTP, 1.2 mM dATP, 0.95 mM dTTP, 0.25 mM dUTP) along with 50 units of Klenow Exo– (NEB) was added, and the reaction was allowed to proceed at 22 °C for 10 min and then at 37 °C for 30 min. The reaction was then heated to 95 °C for 5 min and then chilled rapidly on ice. A further 50 units of Klenow Exo– was added and the reaction was incubated at 22 °C for 10 min and then at 37 °C for 30 min. The reaction was stopped by phenol:chloroform extraction, and unincorporated random hexamers were removed with a gel filtration spin column. The DNA was then fragmented with the use of the wild-type Terminal Labelling Kit (Affymetrix).

Labelling of DNA. Samples to be hybridized on the microarrays (with the exception of full-length nucleosomal DNA fragments) were fragmented with the use of the wild-type Terminal Labelling Kit (Affymetrix) according to instructions. Complementary DNA was prepared and fragmented according to the wild-type double-stranded target assay manual for model organisms (Affymetrix). All DNA fragments were labelled using the wild-type Terminal Labelling Kit (Affymetrix) according to instructions.

ChIP analysis. Analysis of data from ChIP was performed using the Genomics Suite Software from Partek. Two biological replicates for wild-type Isw2 ChIP and Isw2(K215R) ChIP data sets were prepared. Each sample was normalized using quantile normalization. Initial signal intensity was calculated by normalizing the immunoprecipitation signal to that of the control input signal. The ratio of wild-type Isw2 input normalized signal to Isw2(K215R) input normalized signal was then calculated for each of the replicates. Regions of enrichment were identified using Partek software that identifies significant regions on the basis of a *t*-test on a sliding window (250 bp) centred around each probe; this tests the distribution of neighbouring values. Significant regions are defined as contiguous genomic regions that pass the *P*-value threshold ($P = 0.01$) in both samples. Only significant regions enriched in both replicates are used in this study.

RNA analysis. RNA samples hybridized to microarrays were normalized using quantile normalization and were analysed using TAS software (Affymetrix). Two-sample analysis was performed using a bandwidth of 66 bp. RNA harvested form Δ*trf4* yeast was set as the control group and RNA from Δ*trf4*Δ*isw2* was set as the treatment group. Primer extension reactions to map the transcription start sites were carried out using 30 μg of total RNA using the protocol described in ref. 26.